Heterogeneous Catalysis

Supported Au–Cu Bimetallic Alloy Nanoparticles: An Aerobic Oxidation Catalyst with Regenerable Activity by Visible-Light Irradiation**

Yoshitsune Sugano, Yasuhiro Shiraishi,* Daijiro Tsukamoto, Satoshi Ichikawa, Shunsuke Tanaka, and Takayuki Hirai

Aerobic oxidation by a heterogeneous catalyst with molecular oxygen as an oxidant is a significant process for the synthesis of various chemicals.[1] Gold nanoparticles supported on solid supports have been extensively studied as promising catalysts;[2–4] several types of substrates, such as alcohols,[5–7] aldehydes,[8] and hydrocarbons,[9] are oxidized at ca. 393 K. The current mission is the design of Au catalysts that exhibit high activity under milder reaction conditions (room temperature and atmospheric pressure), from the viewpoint of green chemistry.[10, 11]

One powerful approach for the design of a highly active Au catalyst is the creation of alloy particles. Several reports revealed that particles consisting of Au–Pt,[12] Au–Pd,[13] and Au–Ag[14] bimetallic alloys exhibit much higher activity than monometallic Au particles. In particular, Au–Cu alloys have attracted much attention, because of their high activity and the low cost of Cu. Liu et al.[15] reported that Au–Cu alloy particles (ca. 3 nm) supported on mesoporous silica are three times more effective for the aerobic oxidation of carbon monoxide than monometallic Au particles at room temperature. Li et al.[16] and Pina et al.[17] have reported that Au–Cu alloy particles (ca. 3 nm) supported on silica are 1.5 times more effective for the aerobic oxidation of alcohols than Au particles. The enhanced activity of the Au–Cu alloy is believed to be due to the efficient activation of O_2 on the alloy site. The Au–Cu alloys, however, rapidly lose their activity during the reaction, because O_2 oxidizes surface Cu atoms[18] and eliminates alloying effects. The protection of surface Cu atoms from oxidation is therefore a challenge for efficient aerobic oxidation under milder conditions.

Herein, we report that visible-light irradiation ($\lambda > 450$ nm) of Au–Cu alloy particles during reaction suppresses the oxidation of surface Cu atoms and successfully promotes aerobic oxidation without catalyst deactivation. This is triggered through visible light absorption by the surface Au atoms owing to the resonant oscillation of free electrons coupled by light, an effect which is known as localized surface plasmon resonance (SPR).[19] Collective oscillation of e^- on the surface Au atoms reduces the oxidized surface Cu atoms and maintains the Au–Cu alloying effect. Sunlight irradiation also facilitates activity regeneration and promotes aerobic oxidation at room temperature.

Au–Cu alloy nanoparticles were loaded on Degussa P25 TiO_2 (diameter, 24 nm; BET surface area, 57 $m^2 g^{-1}$; anatase/rutile = ca. 83:17) by simultaneous deposition of Au and Cu precursors followed by reduction with H_2.[20–22] TiO_2 was stirred in water (pH 7) with $HAuCl_4$ and $Cu(NO_3)_2$ at 353 K. The obtained powders were reduced with H_2, affording $Au_{1-x}Cu_x$/P25 catalysts as purple powders. The total amount of metals (($Au + Cu$)/P25 × 100) was set at 1 mol%, and x denotes the amount of Cu loaded (x mol% = Cu/TiO_2 × 100). Figure 1a shows a typical transmission electron microscopy (TEM) image of $Au_{0.7}Cu_{0.3}$/P25. Spherical metal par-
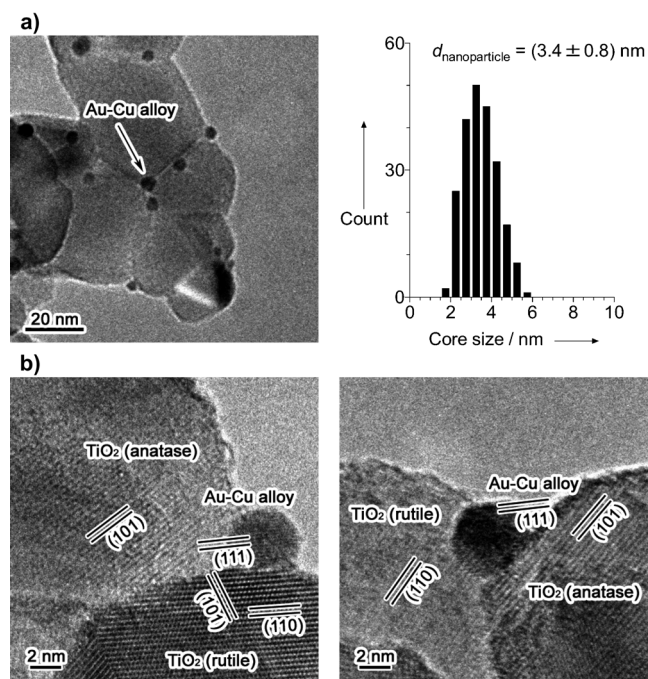
[*] Dr. Y. Sugano, Dr. Y. Shiraishi, Dr. D. Tsukamoto, Prof. T. Hirai
Research Center for Solar Energy Chemistry and Division of Chemical Engineering, Graduate School of Engineering Science, Osaka University, Toyonaka 560-8531 (Japan)
E-mail: shiraish@cheng.es.osaka-u.ac.jp

Dr. S. Ichikawa
Institute for NanoScience Design, Osaka University (Japan)

Dr. S. Tanaka
Department of Chemical, Energy and Environmental Engineering, Kansai University (Japan)

Figure 1. a) Typical TEM image of $Au_{0.7}Cu_{0.3}$/P25 catalyst and size distribution of metal nanoparticles. b) HRTEM image.

ticles with an average diameter of 3.4 nm were observed. As shown in Figure S1 in the Supporting Information, Au_1/P25, $Au_{0.5}Cu_{0.5}$/P25, and Cu_1/P25 contain metal particles with similar diameters (3.8, 3.5, and 3.1 nm, respectively), which indicates that Cu alloying scarcely affects the size of metal particles. As shown in Figure 1b, high-resolution TEM images of the alloy catalyst revealed that metal particles are located at the interface of anatase/rutile TiO_2, as observed for the monometallic Au/P25 catalyst,[23] owing to the strong adhesion of metal particles onto the interface site of TiO_2.[24]

X-ray photoelectron spectroscopy (XPS) of alloy catalysts (Figure S2) shows Au 4f peaks (ca. 82 and 86 eV) and Cu 2p peak (ca. 932 eV).[25] The increase in the amount of Cu shifts the Au peaks to lower binding energy due to the higher electronegativity of Au.[26] The surface Au/Cu molar ratio on $Au_{0.7}Cu_{0.3}$/P25 was determined by XPS analysis to be 2.27. This is similar to the molar ratio of the total amounts of Au and Cu in the catalysts (2.32), as determined by inductively coupled plasma (ICP) analysis and the average Au/Cu molar ratio (2.35) determined by energy-dispersive X-ray spectroscopy (EDX) of metal particles (Figure S3). Moreover, as shown in Figure 1b, the lattice constants calculated from lattice spacing of alloy particles by TEM observation (left: $a = 0.394$ nm), right: $a = 0.396$ nm) are in between the lattice constants for standard Au (JCPDS 04-0784, $a = 0.4079$ nm) and Cu (JCPDS 04-0836, $a = 0.3615$ nm), and are similar to the value calculated based on Vegard's law ($a = 0.3940$ nm). These suggest that Au and Cu components in the alloy are homogeneously mixed. As shown in Figure 2, the diffuse-reflectance UV/Vis spectrum of Au_1/P25 shows a distinctive SPR band at 551 nm. Cu alloying decreases the SPR intensity with a red shift of the band, as is the case for colloidal Au–Cu alloy particles.[27]
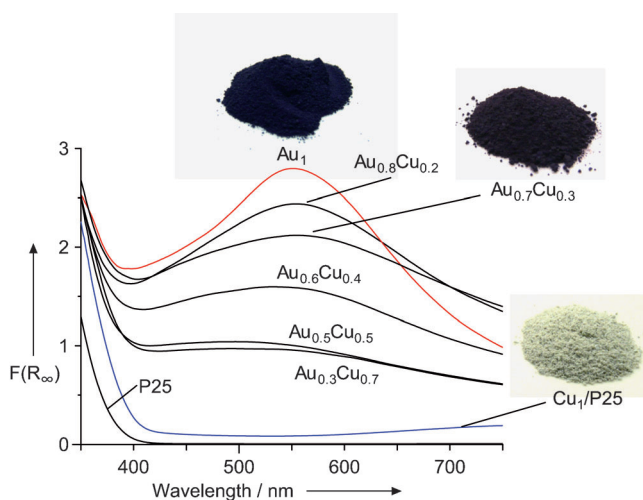

Figure 2. Diffuse-reflectance UV/Vis spectra of the catalysts.

Catalytic activity was tested by the aerobic oxidation of 2-propanol. The reactions were performed by stirring the catalyst (5 mg) in 2-propanol (5 mL) under O_2 atmosphere (1 atm) in the dark or under visible-light irradiation with a Xe lamp ($\lambda > 450$ nm). The temperature of the solution was kept

rigorously at (298 ± 0.5) K with a digitally-controlled water bath. Figure 3 summarizes the amount of acetone produced by 12 h reaction in the dark (black bars) or visible-light
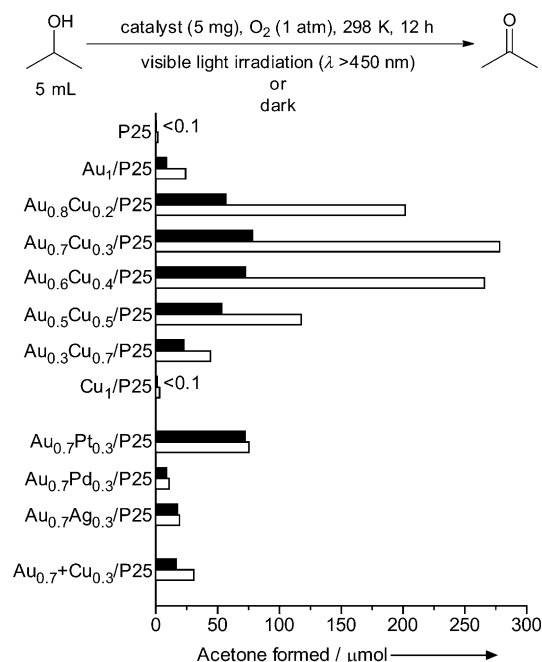

Figure 3. Amount of acetone formed during the aerobic oxidation of 2-propanol in the dark (black bars) or under visible-light irradiation (white bars; $\lambda > 450$ nm; light intensity at 450–800 nm, 16.8 mWcm^{-2}).

irradiation (white bars). Both reactions selectively produced acetone (mass balance $> 99\%$) and little reaction was observed in the absence of O_2. In the dark, bare P25 promotes almost no reaction, but Au_1/P25 produces 8 µmol of acetone. The Au–Cu alloy catalysts exhibit much higher activity owing to the alloying effect. The increase in the amount of Cu enhances the activity, and $Au_{0.7}Cu_{0.3}$/P25 produces the largest amount of acetone (78 µmol). Larger Cu loadings are ineffective, and Cu_1/P25 promotes almost no reaction. These activities of alloy catalysts in the dark are consistent with those observed in early reports.[16,17] The most interesting feature of the alloy catalyst is the significant activity enhancement observed under visible-light irradiation. As indicated by the white bars, the alloy catalysts exhibit enhanced acetone formation. Among them, $Au_{0.7}Cu_{0.3}$/P25 produces the largest amount of acetone (278 µmol), which is nearly four times that obtained in the dark (78 µmol). In contrast, the reaction enhancement of the monometallic Au_1/P25 catalyst by visible-light irradiation is very small, and Cu_1/P25 shows almost no enhancement. These data suggest that Au–Cu alloy catalysts are effective at promoting aerobic oxidation under visible-light irradiation.

As shown in Figure 3, the reaction enhancement by visible-light irradiation is scarcely observed when using the catalysts loaded with Au–Pt, Au–Pd, and Au–Ag alloys. Furthermore, the $Au_{0.7} + Cu_{0.3}$/P25 catalyst prepared by a step-by-step deposition of Au and Cu metals onto the

support (see the Supporting Information) scarcely exhibits reaction enhancement. These findings suggest that homogeneously mixed Au–Cu alloy particles are necessary for this effect.

The enhanced activity of the Au–Cu alloy catalyst is due to visible light reducing the surface Cu atoms that have been oxidized by O_2. This maintains the Au–Cu alloying effect and promotes aerobic oxidation without catalyst deactivation. This is confirmed by the time-dependent change in the amount of acetone formed during aerobic oxidation of 2-propanol with $Au_{0.7}C_{0.3}$/P25. As shown in Figure 4 (●), the
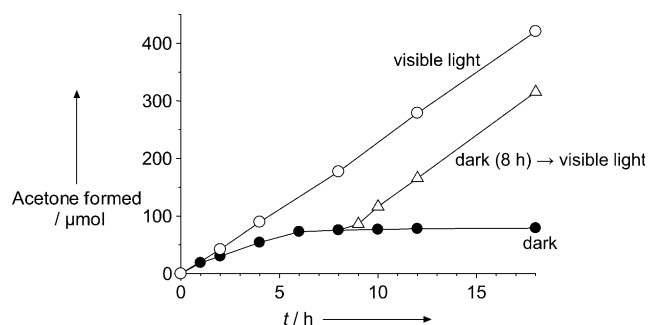
Figure 4. Time-dependent change in the amount of acetone formed by aerobic oxidation of 2-propanol with the $Au_{0.7}Cu_{0.3}$/P25 catalyst under visible-light irradiation (○), in the dark (●), and in the dark for 8 h followed by visible-light irradiation (△). Reaction conditions are identical to those in Figure 3.

reaction in the dark is effective in the early stage (ca. 2 h), but the activity decreases with time. This is because the surface Cu atoms are oxidized by O_2 during the reaction, thus eliminating the alloying effect.[16] In contrast, under photo-irradiation (○), the rate of acetone formation in the early stage is similar to that obtained in the dark, but the activity is maintained even after 18 h. This suggests that visible-light irradiation suppresses catalyst deactivation. To further clarify this effect, the reaction was carried out in the dark for 8 h and continued under visible-light irradiation (△). The catalytic activity is successfully regenerated by photoirradiation.

Activity regeneration by visible-light irradiation is due to the reduction of oxidized surface Cu atoms with alcohol as an electron donor. ESR analysis confirms this. Figure 5a shows the spectrum of $Au_{0.7}Cu_{0.3}$/P25 measured at 77 K after exposure to O_2 in the dark. Strong signals, which are assigned to Cu^{2+}, are observed at $g_\perp = 2.03$–2.06,[18] indicating that surface Cu atoms are oxidized by O_2. As shown in Figure 5b, visible-light irradiation of sample (a) does not show any spectral change. As shown in Figure 5c, exposure of sample (b) to 2-propanol (10 Torr) in the dark still does not show spectral change. However, as shown in Figure 5d, visible-light irradiation of sample (c) leads to complete disappearance of the Cu^{2+} signals. GC analysis of the sample detects the formation of acetone and water. This suggests that visible-light irradiation of the alloy catalyst reduces oxidized surface Cu atoms with alcohol as an electron donor.

The effectiveness of the reduction of oxidized surface Cu atoms depends on the amount of Au in the alloy. As shown in
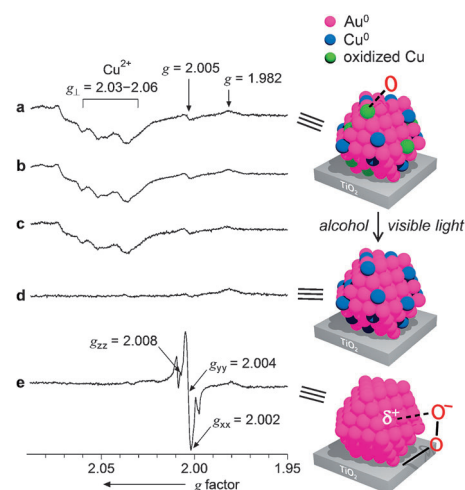

Figure 5. ESR spectra of $Au_{0.7}Cu_{0.3}$/P25 samples (a–d) and a Au_1/P25 sample (e) measured at 77 K. a) The $Au_{0.7}Cu_{0.3}$/P25 catalyst was treated with O_2 (20 Torr) for 3 h in the dark. b) Sample (a) was irradiated by visible light for 3 h. c) 2-Propanol (10 Torr) was added to sample (b) in the dark. d) Sample (c) was irradiated by visible light for 3 h. e) The Au_1/P25 catalyst was treated with O_2 (20 Torr) for 3 h and irradiated by visible light for 3 h. The $g = 2.005$ signal is due to the electrons trapped by oxygen vacancy site of TiO_2, and the $g = 1.982$ signal is due to the Ti^{3+} site on TiO_2.[22]

Figure S4, visible-light irradiation of $Au_{0.3}Cu_{0.7}$/P25 with a lower amount of Au shows a much lower decrease in the Cu^{2+} signal than that of $Au_{0.7}Cu_{0.3}$/P25. Moreover, Cu_1/P25 exhibits almost no signal decrease. These tendencies are consistent with the SPR intensity of the catalysts (Figure 2), suggesting that the reduction of Cu^{2+} is promoted by the light absorption of surface Au species in the alloy. This is further confirmed by the action spectrum for aerobic oxidation of 2-propanol with $Au_{0.7}Cu_{0.3}$/P25 obtained by irradiation of monochromatic light. As shown in Figure 6, a good correlation is observed between the SPR band of the catalyst and the apparent quantum yield for acetone formation (Φ_{AQY}). This suggests that plasmon-activated surface Au atoms indeed promote the reduction of oxidized surface Cu atoms.

As shown in Figure 7, plasmon-activated surface Au atoms promote the intraband transition of $6\,sp$ e^-.[28] The
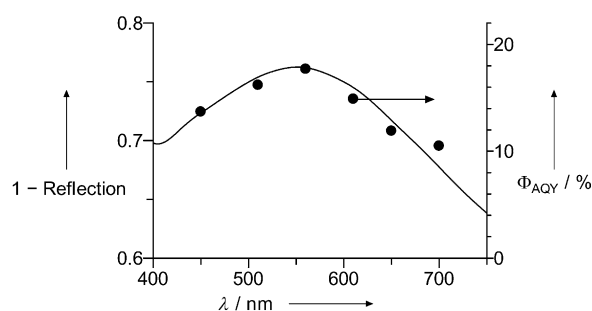

Figure 6. Action spectrum for aerobic oxidation of 2-propanol on the $Au_{0.7}Cu_{0.3}$/P25 catalyst. The apparent quantum yield for acetone formation (Φ_{AQY}) was calculated with the following equation: Φ_{AQY} (%) $= [\{(Y_{vis} - Y_{dark}) \times 2\}/(\text{photon number entered into the reaction vessel})] \times 100$, where Y_{vis} and Y_{dark} are the amounts of acetone formed (µmol) under light irradiation and dark conditions, respectively.
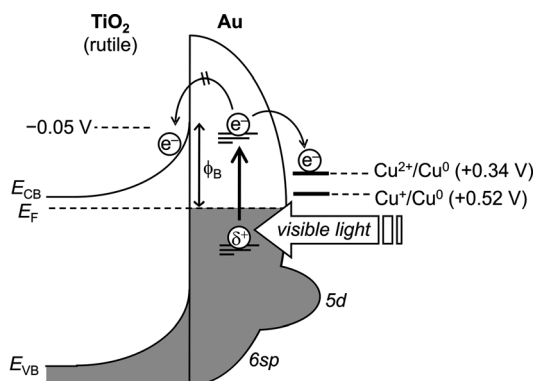
Figure 7. Possible energy diagram (vs. NHE) for plasmon-activated AuCu/P25 catalysts under visible-light irradiation.

electrons are transferred to the adjacent oxidized Cu atoms to reduce them. As we have reported earlier,[23] visible-light irradiation of monometallic Au particles loaded onto TiO_2 transfers electrons to the TiO_2 conduction band, where the plasmon-activated e^- overcomes the Schottky barrier (φ_B) created at the Au/TiO_2 heterojunction.[29] As shown in Figure 5e, visible-light irradiation of Au_1/P25 with O_2 generates oxygen anion ($g_{xx} = 2.002$, $g_{yy} = 2.004$, $g_{zz} = 2.008$). This suggests that a plasmon-activated e^- on the surface Au atom is indeed transferred to the TiO_2 conduction band and reduces O_2 there.[23] In contrast, as shown in Figure 5b, visible-light irradiation of $Au_{0.7}Cu_{0.3}$/P25 with O_2 does not produce oxygen anions. This suggests that e^- transfer to the TiO_2 conduction band does not occur in the alloy system. As shown in Figure 7, the potential of φ_B for TiO_2 (rutile) is located at -0.05 V (vs. NHE)[30] and is more negative than the reduction potentials of Cu^+ ($Cu^+ + e^- = Cu^0$; 0.52 V) and Cu^{2+} ($Cu^{2+} + 2e^- = Cu^0$; 0.34 V).[31] Plasmon-activated electrons are therefore preferentially transferred to oxidized surface Cu atoms. These results suggest that e^- transfer from plasmon-activated surface Au atoms facilitates the successful reduction of oxidized surface Cu atoms.

Aerobic oxidation on the Au–Cu alloy occurs as shown in Scheme 1 A. a) The alloy site activates O_2 and produces an anionic oxygen species.[6] b) This attracts the H atom of the alcohol and produces an alcoholate. c) Subsequent H atom removal gives the corresponding carbonyl product. As shown in Scheme 1 B, d) parts of the surface Cu atoms are oxidized by O_2 during the reaction. e) Plasmon activation of surface Au atoms by visible light reduces the Cu atoms through transfer of activated electrons. f) The resulting positive charge on the Au atoms oxidizes alcohol and produces the carbonyl product and water. The regeneration cycle (B) successfuly reduces the oxidized surface Cu atoms and allows promotion of catalytic cycle (A).

Note that the activity of the Au–Cu alloy depends on the metal oxide support. As shown in Figure S5, the P25 TiO_2 support exhibits the highest activity both in the dark and under visible-light irradiation. This is probably because, as observed in related systems,[32–34] strong adhesion of Au–Cu alloy on the P25 TiO_2 surface[23,24] leads to efficient electron transfer from the support to particles and increases the electron density of alloy particles. This may result in the
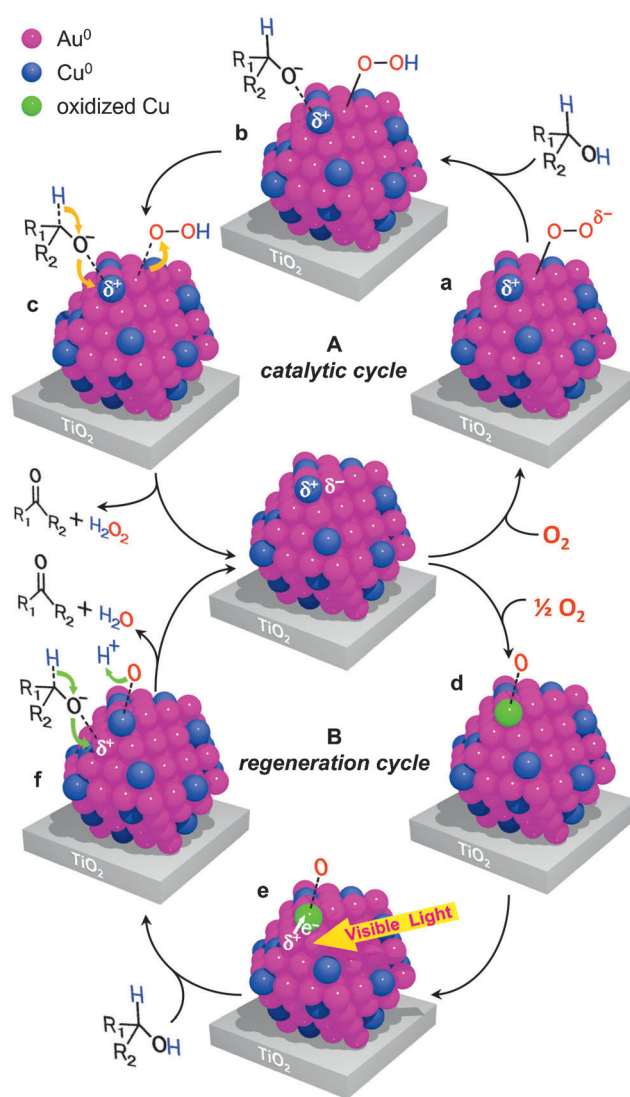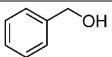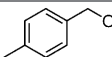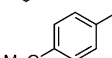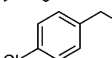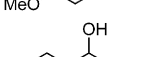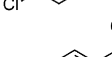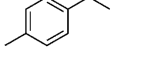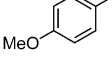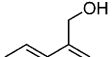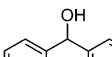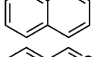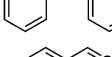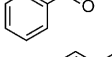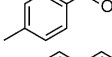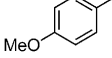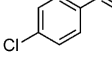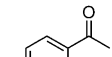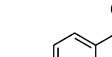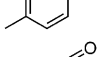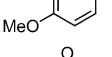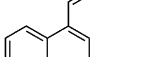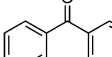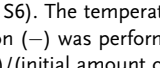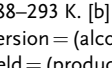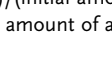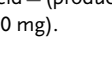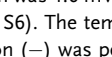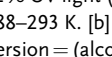

Scheme 1. Proposed mechanism for the A) catalytic cycle for aerobic oxidation of alcohol on AuCu/P25 catalyst, and B) regeneration cycle for the reduction of oxidized surface Cu atoms.

efficient activation of O_2[35] and enhanced transfer of plasmon-activated electrons to the oxidized surface Cu atoms.

The Au–Cu alloy catalyst promotes aerobic oxidation even under sunlight irradiation at ambient temperature. Table 1 shows the results for the oxidation of benzylic alcohols with $Au_{0.7}Cu_{0.3}$/P25 under sunlight, where the temperature of the solution during the reaction was 288–293 K. Sunlight exposure selectively oxidizes these benzylic alcohols to the corresponding carbonyl products with very high yields (71–88%). These yields are much higher than those obtained in the dark at 293 K. This suggests that the alloy catalyst is successfully regenerated, even by sunlight, and is effective at promoting aerobic oxidation.[36]

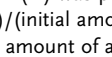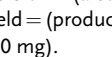In summary, we show that supported Au–Cu alloy nanoparticles promote aerobic oxidation under visible light. The surface Cu atoms oxidized by O_2 during the reaction are successfully reduced by plasmon-activated Au atoms. This maintains the alloying effect and promotes aerobic oxidation. Sunlight irradiation is also effective for activity regeneration.

Table 1: Effect of sunlight exposure on aerobic oxidation of alcohols with the $Au_{0.7}Cu_{0.3}$/P25 catalyst.[a]

Entry	Substrate	Sunlight[b]	Conv. [%][c]	Product	Yield [%][d]
1		+	84		84
2		−	18		18
3		+	74		74
4		−	17		16
5		+	75		75
6		−	20		20
7		+	72		71
8		−	16		16
9		+	79		78
10		−	21		20
11[e]		+	82		81
12[e]		−	32		31
13		+	88		88
14		−	45		44
15		+	81		80
16		−	11		10

[a] Reaction conditions: toluene (5 mL), alcohol (50 µmol), catalyst (20 mg), O_2 (1 atm), exposure time (6 h). The light intensity at 300–800 nm was 4.6 mW cm^{-2}, which involves only 2% UV light ($\lambda < 400$ nm; Figure S6). The temperature of solution was 288–293 K. [b] The dark reaction (−) was performed at 293 K. [c] Conversion = (alcohol converted)/(initial amount of alcohol) × 100. [d] Yield = (product formed)/(initial amount of alcohol) × 100. [e] Catalyst (40 mg).

The catalytic system presented here, which enables activity regeneration by the plasmon activation of Au atoms by visible light, may contribute to the design of more efficient catalytic systems and may provide a new strategy for the development of green organic transformations using sunlight.

[1] R. A. Sheldon, I. W. C. E. Arends, A. Dijksman, *Catal. Today* **2000**, *57*, 157–166.
[2] M. Haruta, *Nature* **2005**, *437*, 1098–1099.
[3] A. A. Herzing, C. J. Kiely, A. F. Carley, P. Landon, G. J. Hutchings, *Science* **2008**, *321*, 1331–1335.
[4] C. D. Pina, E. Falletta, L. Prati, M. Rossi, *Chem. Soc. Rev.* **2008**, *37*, 2077–2095.
[5] A. Abad, P. Concepcion, A. Corma, H. García, *Angew. Chem.* **2005**, *117*, 4134–4137; *Angew. Chem. Int. Ed.* **2005**, *44*, 4066–4069.
[6] T. Ishida, M. Nagaoka, T. Akita, M. Haruta, *Chem. Eur. J.* **2008**, *14*, 8456–8460.
[7] A. Abad, A. Corma, H. García, *Chem. Eur. J.* **2008**, *14*, 212–222.
[8] A. Corma, M. E. Domine, *Chem. Commun.* **2005**, 4042–4044.
[9] M. Turner, V. B. Golovko, O. P. H. Vaughan, P. Abdulkin, A. Berenguer-Murcia, M. S. Tikhov, B. F. G. Johnson, R. M. Lambert, *Nature* **2008**, *454*, 981–984.
[10] T. Mitsudome, A. Noujima, T. Mizugaki, K. Jitsukawa, K. Kaneda, *Adv. Synth. Catal.* **2009**, *351*, 1890–1896.
[11] S. Kim, S. W. Bae, J. S. Lee, J. Park, *Tetrahedron* **2009**, *65*, 1461–1466.
[12] Y. Shen, S. Zhang, H. Li, Y. Ren, H. Liu, *Chem. Eur. J.* **2010**, *16*, 7368–7371.
[13] K. Kaizuka, H. Miyamura, S. Kobayashi, *J. Am. Chem. Soc.* **2010**, *132*, 15096–15098.
[14] N. K. Chaki, H. Tsunoyama, Y. Negishi, H. Sakurai, T. Tsukuda, *J. Phys. Chem. C* **2007**, *111*, 4885–4888.
[15] X. Liu, A. Wang, X. Wang, C. Y. Mou, T. Zang, *Chem. Commun.* **2008**, 3187–3189.
[16] W. Li, A. Wang, X. Liu, T. Zhang, *Appl. Catal. A* **2012**, *433–434*, 146–151.
[17] C. D. Pina, E. Falletta, M. Rossi, *J. Catal.* **2008**, *260*, 384–386.
[18] X. Liu, A. Wang, L. Li, T. Zhang, C. Y. Mou, J. F. Lee, *J. Catal.* **2011**, *278*, 288–296.
[19] P. K. Jain, X. Huang, I. H. El-Sayed, M. A. El-Sayed, *Acc. Chem. Res.* **2008**, *41*, 1578–1586.
[20] Y. Shiraishi, M. Ikeda, D. Tsukamoto, S. Tanaka, T. Hirai, *Chem. Commun.* **2011**, *47*, 4811–4813.
[21] Y. Shiraishi, Y. Takeda, Y. Sugano, S. Ichikawa, S. Tanaka, T. Hirai, *Chem. Commun.* **2011**, *47*, 7863–7865.
[22] M. Okumura, J. M. Coronado, J. Soria, M. Haruta, J. C. Conesa, *J. Catal.* **2001**, *203*, 168–174.
[23] D. Tsukamoto, Y. Shiraishi, Y. Sugano, S. Ichikawa, S. Tanaka, T. Hirai, *J. Am. Chem. Soc.* **2012**, *134*, 6309–6315.
[24] T. Akita, P. Lu, S. Ichikawa, K. Tanaka, M. Haruta, *Surf. Interface Anal.* **2001**, *31*, 73–78.
[25] S. Albonetti, T. Pasini, A. Lolli, M. Blosi, M. Piccinini, N. Dimitratos, J. A. Lopez-Sanchez, D. J. Morgan, A. F. Carley, G. J. Hutchings, F. Cavani, *Catal. Today* **2012**, *195*, 120–126.
[26] A. Zwijnenburg, A. Goossens, W. G. Sloof, M. W. J. Crajé, A. M. Kraan, L. J. Jongh, M. Makkee, J. A. Moulijn, *J. Phys. Chem. B* **2002**, *106*, 9853–9862.
[27] N. E. Motl, E. Ewusi-Annan, I. T. Sines, L. Jensen, R. E. Schaak, *J. Phys. Chem. C* **2010**, *114*, 19263–19269.
[28] H. Zhu, X. Chen, Z. Zheng, X. Ke, E. Jaatinen, J. Zhao, C. Guo, T. Xie, D. Wang, *Chem. Commun.* **2009**, 7524–7526.
[29] E. W. McFarland, J. Tang, *Nature* **2003**, *421*, 616–618.
[30] H. P. Maruska, A. K. Ghosh, *Sol. Energy* **1978**, *20*, 443–458.
[31] Y. Nosaka, S. Takahashi, H. Sakamoto, A. Y. Nosaka, *J. Phys. Chem. C* **2011**, *115*, 21283–21290.
[32] M. S. Chen, D. W. Goodman, *Catal. Today* **2006**, *111*, 22–33.
[33] T. Minato, T. Susaki, S. Shiraki, H. S. Kato, M. Kawai, K. Aika, *Surf. Sci.* **2004**, *566–568*, 1012–1017.
[34] S. Arrii, F. Morfin, A. J. Renouprez, J. L. Rousset, *J. Am. Chem. Soc.* **2004**, *126*, 1199–1205.
[35] H. Tsunoyama, N. Ichikuni, H. Sakurai, T. Tsukuda, *J. Am. Chem. Soc.* **2009**, *131*, 7086–7093.
[36] The aerobic oxidation of aliphatic alcohols, especially primary alcohols, was unsuccessful owing to their low reactivity and the subsequent esterification of their aldehyde products (Ref. [11]). As shown in Table S1, 1-propanol and 1-hexanol exhibit reactivities and selectivities lower than those of benzylic alcohols (Table 1), although visible-light irradiation enhances the reaction owing to the plasmon-induced catalyst regeneration.